8018 *Macromolecules* **2010**, *43*, 8018–8025
DOI: 10.1021/ma1014325

Macromolecules
ARTICLE

Synthesis of Linear, H-Shaped, and Arachnearm Block Copolymers By Tandem Ring-Opening Polymerizations

Louis M. Pitet,[†] Bradley M. Chamberlain,[‡] Adam W. Hauser,[†] and Marc A. Hillmyer*[,†]

[†]*Department of Chemistry, University of Minnesota, 207 Pleasant St. SE, Minneapolis, Minnesota 55455-0431, and* [‡]*Department of Chemistry, Luther College, 700 College Drive, Decorah, Iowa 52101*

Received June 28, 2010; Revised Manuscript Received July 27, 2010

ABSTRACT: We have demonstrated the two-stage preparation of block polymers with various architectures containing mechanistically incompatible monomers. Three new monounsaturated chain transfer agents (CTAs) were synthesized containing two, four, or eight hydroxyl groups and used for the preparation of telechelic poly(*cis*-cyclooctene) (PCOE) by ring-opening metathesis polymerization (ROMP). We observed excellent end-group fidelity along with well-controlled molecular weights based on the initial monomer to CTA ratio. Each PCOE was subsequently used as a macroinitiator for the polymerization of D,L-lactide to produce compositionally controlled B_xAB_x block polymers with linear ($x = 1$), H-shaped ($x = 2$), and arachne(spider)arm ($x = 4$) architectures. Block polymers were prepared containing PLA weight fractions (w_L) ranging from 0.25−0.85. This report significantly expands on the method of combining mechanistically incompatible monomers via tandem polymerizations by introducing branched architectures that can facilitate specific property tailoring.

Precise control over chemical composition and chain architecture in block polymers has been widely achieved due to the ready accessibility of various controlled polymerization techniques. Combining mechanistically incompatible monomers into these hybrid macromolecules remains an attractive approach to the development of new materials with a broad array of physical properties.[1] The preparation of block copolymers containing mechanistically incompatible monomers is no longer a curiosity; the emergence of controlled free radical polymerizations and the development of tolerant and selective catalysts for various ring-opening polymerizations have provided access to a range of fascinating hybrid materials.[2] As a pertinent example, combining ring-opening metathesis polymerization (ROMP) with other polymerization mechanisms can be achieved by polymerizing a cyclic olefin in the presence of an acyclic olefin that acts as a chain transfer agent (CTA) and bears one or more functional groups capable of initiating the growth of another polymer.[3]

Block polymers have proven quite useful for many applications due to the array of nanostructures they can adopt.[4] Moreover, block polymers with branched architectures have attracted attention based largely on the interesting bulk mechanical and morphological behavior compared to their linear counterparts.[5] Branched block copolymers with arms of one macromolecule linked to a different macromolecule, so-called mikto(mixed)arm block polymers, have been studied extensively, and synthetic pathways to these fascinating molecules have been reviewed.[6] In particular, symmetrical linear−branched hybrid block copolymers with the general architecture B_xAB_x have been synthesized from mechanistically incompatible monomers. For example, Sill and Emrick described BAB dendritic−linear hybrids by using a symmetric monounsaturated macromolecular CTA containing poly(phenyl ether) dendritic moieties in the ROMP of *cis*-cyclooctene (**COE**).[7] This general method can be extended by using end-groups capable of initiating polymerization of another monomer, as demonstrated with linear PDMS prepared anionically and modified to incorporate two hydroxyl end-groups per chain end that could be subsequently used to initiate ring-opening transesterification polymerization (ROTEP) of ε-caprolactone.[8] Similarly, Pan and co-workers polymerized styrene using atom-transfer radical polymerization (ATRP) initiated from a symmetric difunctional species followed by postpolymerization functionalization to afford a tetrahydroxy PS macroinitiator for ring-opening polymerization of D,L-lactide (**LA**), resulting in B_2AB_2 block polymers.[9] More recently, Xie and co-workers described an approach to AB_2 miktoarm block copolymers combining living ROMP with ATRP.[10] Poly(7-oxanorborn-5-ene) produced using the first generation Grubbs catalyst was end-functionalized with a dibromo moiety by terminating with a symmetric CTA. Branched amphiphilic block copolymers were achieved by subsequent polymerization of 2-(dimethylamino)ethyl methacrylate. As a final example, Hedrick and co-workers prepared linear poly(ethylene oxide) (PEO) having either one or two primary amines per chain end and demonstrated the ability of each amine to initiate two polylactide (PLA) chains using an organocatalyst, thus forming H-shaped and eight-arm block polymers, respectively.[11] This is the only example of well-defined B_4AB_4 block copolymers we have found in the literature. Given the center segment in such materials is flanked by a set of four arms, we refer to these as arachne(spider)arm block copolymers.

We recently reported the preparation of linear BAB triblocks by combining hydroxyl initiated ROTEP of **LA** from the termini of telechelic poly(1,5-cyclooctadiene) (PCOD) prepared using ROMP.[12] However, the methodology employed an acetoxy protected CTA, which necessitated a somewhat tedious post-ROMP deprotection step.[13] Here we report the synthesis of three new symmetrical hydroxyl bearing CTAs with functionalities of 2, 4, and 8 through modification of commercially available *cis*-2-butene-1,4-diol (**C2B**). These CTAs undergo secondary metathesis during ROMP of *cis*-cyclooctene (**COE**) and end-group fidelity was confirmed by the successful subsequent polymerization of D,L-lactide from the poly(*cis*-cyclooctene) (PCOE) macroinitiators.

*To whom correspondence should be addressed. E-mail: hillmyer@umn.edu.

 Published on Web 09/01/2010

Using ROMP with the multifunctional CTAs allows for direct preparation of the branched block copolymers having the B_xAB_x architectures as illustrated in Figure 1.

Collectively, we present in this report new methods for (1) the utilization of hydroxyl-bearing chain transfer agents for ROMP that do not require postpolymerization deprotection, (2) the straightforward and direct synthesis of a set of architecturally diverse block polymers, and (3) the marriage of two versatile ring-opening polymerizations that promise ready access to numerous hybrid materials.

Results and Discussion

Synthesis of New CTAs. Hydroxyl-telechelic polymers can be routinely synthesized via ROMP of cyclic olefins in the presence of a suitably functionalized CTA.[12−15] Hydroxyl functionality has been achieved both directly and indirectly using **C2B**[f4b] and protected analogues of *cis*-substituted CTAs,[3f,13,14,16] respectively, which practically yield polymers with number-average functionality (F_n) = 2.[17] However, particular difficulty is encountered during the direct ROMP of cyclic olefins with **C2B**; low yields and poorly controlled molecular weights have been observed presumably from catalyst deactivation.

There are no reports describing the synthesis of linear polymers by ROMP with multiple hydroxyl groups per chain end. As such, we synthesized three new CTAs that lead to hydroxyl-telechelic polymers with well-controlled molecular weights and variable numbers of hydroxyl groups per chain end when polymerized with the cyclic olefin **COE** catalyzed by the second generation Grubbs catalyst (**G2**). Symmetric CTAs with two, four, or eight hydroxyl groups per molecule were synthesized starting from commercially available **C2B** according to Scheme 1.

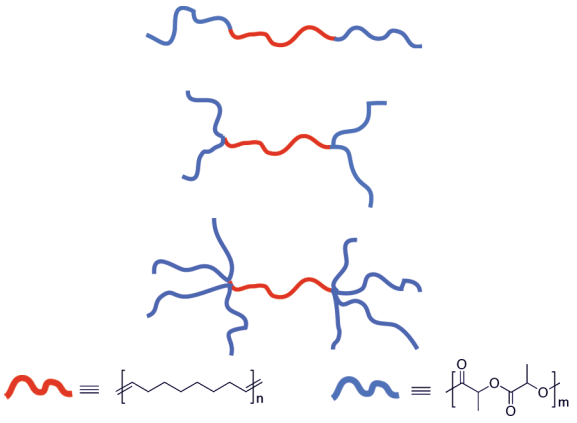

Figure 1. Schematic representation of the block copolymer architectures prepared in this work containing poly(*cis*-cyclooctene) [red] and poly(D,L-lactide) [blue] components.

Compound **1** was prepared because we desired a CTA that would lead directly to hydroxyl-telechelic ROMP products in a controlled manner, in one polymerization step, and without post-polymerization modification as was necessary using 1,4-diacetoxy-*cis*-2-butene as a CTA.[12,13a,13c,18] For practical purposes, we also sought a difunctional CTA that could be readily prepared from commercially available sources.

Compound **1** was prepared by reacting **C2B** with 2.5 equiv of **LA** catalyzed by tin(II) 2-ethylhexanoate [$Sn(Oct)_2$]. The resulting product is actually a mixture of oligomers due to simultaneous ring-opening of **LA** by both **C2B** and the secondary hydroxyl that results from ring-opened **LA**. The average molecular weight of the CTA **1** mixture was estimated from ^{1}H NMR spectroscopy and supported by elemental analysis and mass-spectrometry (see Supporting Information, Figure S1). The reaction conditions also facilitate transesterification to some extent according to the mass-spectrum obtained from electrospray ionization; hence, the mixture consists of **C2B** with different oligomeric lactic acid units [$-C(O)C(CH_3)O- \equiv C_3$]; the average chemical makeup is reflected in Scheme 1, where the average of $(p+q) \approx 3.5$ This value is slightly larger than that expected for quantitative initiation and conversion of lactide ring-opening [$(p+q)_{theo} \approx 3$], which would be consistent with incomplete incorporation of the **C2B**. (See Supporting Information for further description). The critical characteristic for utility during ROMP relies on the retention of the alkene in the *cis* configuration. A high retention rate is suggested by ^{1}H and ^{13}C NMR and IR spectroscopy (see Figure S2, S3, S5 in Supporting Information). The most convincing evidence for *cis* configuration comes from the accuracy with which molecular weight can be targeted based on the estimated CTA molecular weight and the ratio [**COE**]:[CTA]; the *trans* version of the CTA is expected to have lower reactivity with the **G2** catalyst.

The esterification of **2**[19] with **C2B** using dicyclohexylcarbodiimide (**DCC**) followed by deprotection of the cyclic acetal gives **3** in high yield. The first generation dendritic product formed by coupling **2** with the benzyl-ester protected derivative of bisMPA is a common building block in the preparation of hyperbranched polyesters; combining this methodology with the ROTEP of **LA** and ε-caprolactone resulted in degradable hyperbranched polyesters with interesting properties.[19,20] Removal of the benzyl group by hydrogenolysis gives the acetal protected first generation dendrimer of bisMPA **4** in nearly quantitative yield. Analogous esterification of **4** with **C2B** and

Scheme 1. Synthesis of Difunctional (1), Tetrafunctional (3), and Octafunctional (5) CTAs via Modification of *cis*-2-Butene-1,4-diol

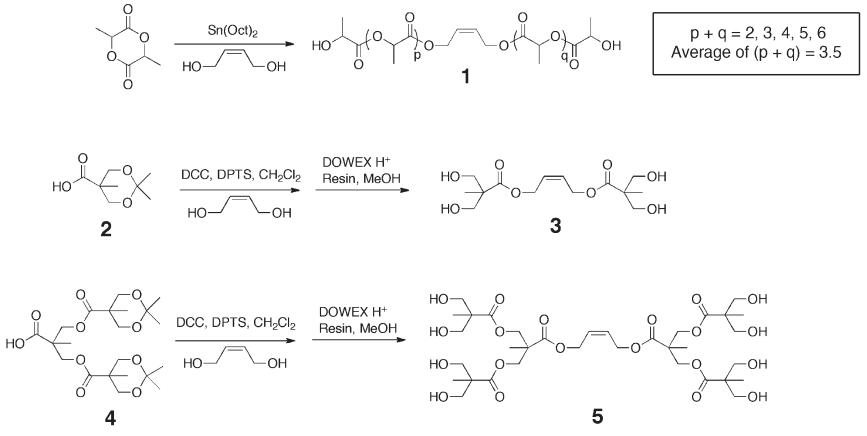

Scheme 2. Polymerization of Cyclooctene in the Presence of CTAs 1, 3, and 5 To Yield Multiply Functional Hydroxyl-Telechelic PCOE

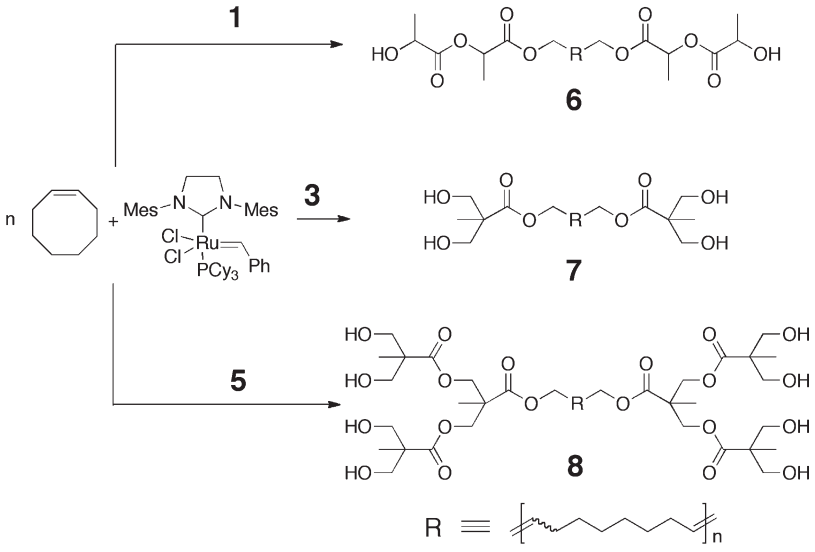

Table 1. Molecular Characteristics of PCOE Homopolymers

sample ID	M_n[a](calc) (kg mol^{-1})	M_n[b](NMR) (kg mol^{-1})	M_n[c] (LS) (kg mol^{-1})	PDI[d] (SEC)	dn/dc[e](LS) (mL/g)
HO−C−OH	22.5	22.5	24.2	1.70	0.113
HO_2−C−OH_2	22.3	22.8	25.5	1.71	0.112
HO_4−C−OH_4	25.0	27.7	30.5	1.88	0.109

[a]Calculated from the initial ratio of monomer to chain transfer agent; the molar mass of the monomer and chain transfer agent are included. [b]Calculated from the relative intensities of signals in the ^{1}H NMR spectra corresponding to the end group and monomer assuming no nonfunctional end groups. [c]Measured using a light scattering detector on an SEC with THF eluant at 30 °C. [d]Measured using and RI detector on an SEC with $CHCl_3$ eluant at 35 °C. [e]Calculated from the THF SEC analysis assuming 100% mass recovery.

subsequent acid-catalyzed deprotection of the cyclic acetal yields CTA **5**. Experimental details are provided in the Supporting Information along with characterization of the CTAs by ^{1}H and ^{13}C NMR spectroscopy, 2D-COSY NMR and IR spectroscopy, mass spectrometry and elemental analysis.

ROMP of COE in the Presence of CTAs 1, 3, and 5. Each of the new CTAs was used in the ROMP of **COE** to produce hydroxyl-telechelic PCOE with variable functionality as illustrated in Scheme 2. Polymerization in the presence of **1** provides PCOE **6** with a target $F_n = 2$. Likewise, CTA **3** and **COE** gives a targeted $F_n = 4$ in the resulting telechelic PCOE homopolymer **7**, and finally polymerization of **COE** in the presence of CTA **5** provides PCOE **8** with a target $F_n = 8$. A catalytic quantity of **G2** ([**COE**]:[Ru] ≈ 20 000) facilitates simultaneous ring-opening and cross-metathesis, and the molecular mass of the PCOE homopolymer is controlled by the molar ratio [**COE**]:[CTA] (such a low level of catalyst has little bearing on the number-average degree of polymerization or average functionality).

Hydroxyl-telechelic PCOE was prepared using CTAs **1** and **3** with a ratio [**COE**]:[CTA] = 200 for which the theoretical PCOE molar masses ($M_{n,calc}$) are 22.5 and 22.3 kg mol^{-1}, respectively. For the case of CTA **5** we used [**COE**]:[**5**] = 220, giving $M_{n,calc} = 25.0$ kg mol^{-1}. Experimentally determined molecular characteristics for the three polymers are provided in Table 1; the polymers are identified as $(HO)_x$−C−$(OH)_x$, where x is the number of hydroxyl groups per chain end. For each end-functionalized homopolymer, the relative intensity of the end-group and monomer signals in the ^{1}H NMR spectra were consistent with nearly quantitative incorporation of the CTAs. This also suggests excellent tolerance of **G2** to the hydroxyl functional groups present in the CTAs **1**, **3**, and **5** during ROMP. Apparently, the proximity of the hydroxyl group to the reactive site in **C2B** (allylic position) causes difficulty in controlling the molecular weight, presumably due to deactivation of the catalyst. The CTAs presented in this work place the hydroxyl group adequately far from the olefin in order to sustain activity and prevent deactivation.[21]

Figure 2a shows the ^{1}H NMR spectrum for the HO−C−OH (Table 1) sample of PCOE derived from CTA **1**. For each sample of PCOE, regardless of which CTA was used, the repeat unit signals appear in identical positions and nearly identical ratios of *cis* to *trans* (∼1:8) configurations were observed. Figure 2b, c, and d show magnified portions of the ^{1}H NMR spectra for PCOE derived from CTAs **1**, **3**, and **5**, respectively. The ^{1}H NMR signals associated with the allylic methylene protons adjacent to the ester on the end-groups of the different PCOE samples invariably appear at 4.6 and 4.7 ppm for the *trans* and *cis* configurations, respectively. The relative intensity of the *trans* and *cis* signals associated with the methylene protons on the end groups is consistent between samples and is also consistent with the ratio in the repeat units. These observations are consistent with a strong preference for metathesis to result in the *trans* configuration during ROMP of **COE** and cross-metathesis with PCOE.

Synthesis of Polycyclooctene−Polylactide Block Copolymers. The three new CTAs described above lead to hydroxyl-telechelic polymers with well-controlled molecular weights and variable number of hydroxyl-groups per chain end; molecular weight can be modulated by changing the concentration of the CTA relative to monomer in the polymerization feed (see Table S1 in Supporting Information). The hydroxyl-telechelic PCOE samples shown in Table 1 were used to prepare symmetric BAB-type linear, H-shaped, and arachnearm block copolymers by initiating the ring-opening polymerization of D,L-lactide from the PCOE macroinitiators **6**, **7**, and **8**, respectively (Scheme 3). We chose the catalyst Sn(Oct)$_2$, relying on the well-established molecular weight control, commercial availability, and low loading ratios necessary during **LA** polymerization.

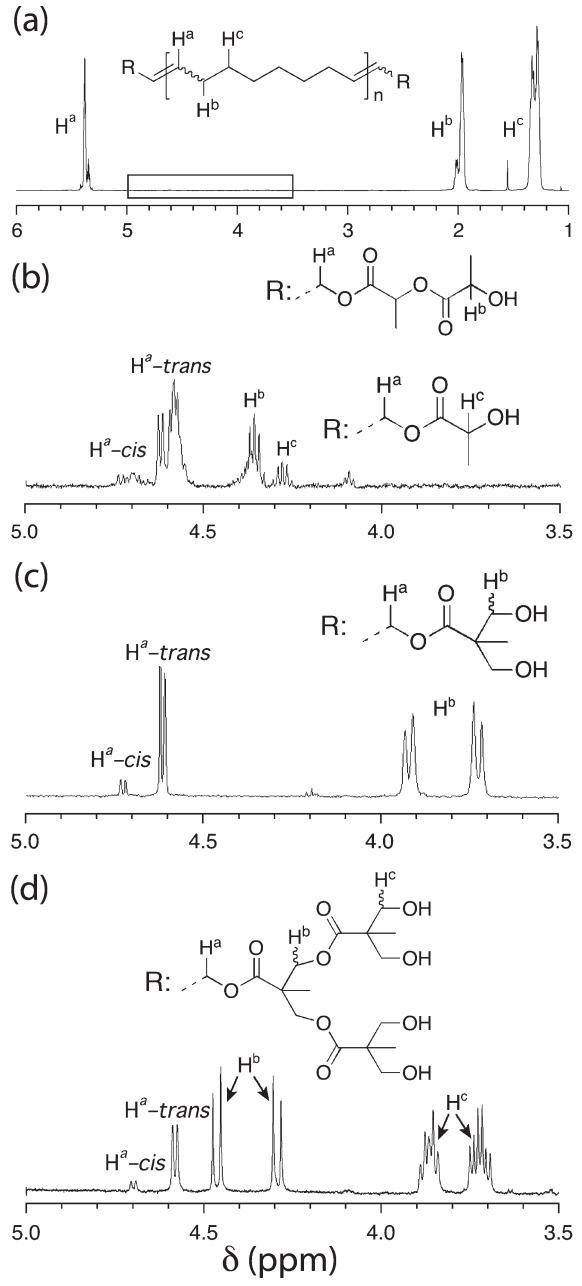

Figure 2. ^{1}H NMR spectra for a representative PCOE homopolymer (a) showing the repeat unit signals and magnified portions showing the respective end-group signals for polymers prepared from CTAs (b) **1** [difunctional], (c) **3** [tetrafunctional], and (d) **5** [octafunctional].

Four separate block polymers with different compositions were prepared from each hydroxyl-telechelic PCOE macroinitiator. Block polymers with PLA weight fractions (w_L) approximately equal to 0.25, 0.45, 0.65, and 0.85 were prepared totaling 12 samples. The molecular characteristics of these samples were evaluated by ^{1}H NMR spectroscopy and SEC with a multiangle laser light scattering (MALLS) detector and are summarized in Table 2. The samples are labeled as L_xCL_x [$\#_x-\#-\#_x$] where the subscript "x" specifies the number of PLA arms emanating from the branching junction between blocks (number is omitted when $x = 1$) and the # is the average molecular weight of the respective block in kg mol^{-1} assuming each hydroxyl group initiated the polymerization of lactide. The molar mass of the block copolymers were determined using the weight fractions calculated from NMR spectroscopy combined with the molar mass of

Scheme 3. Synthesis of Block Copolymers from PCOE Macroinitiators 6, 7, and 8 To Prepare Linear (9), H-Shaped (10), and Arachnearm (11) Architectures

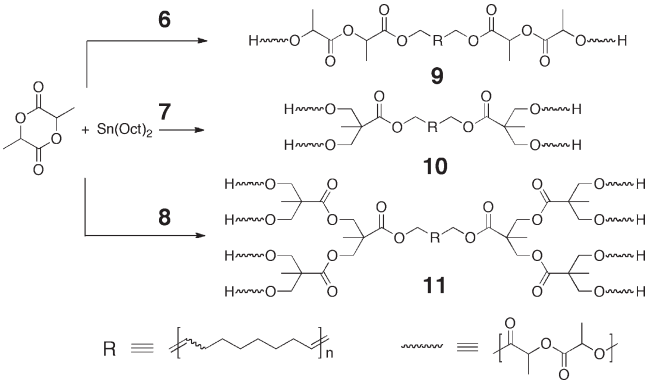

the hydroxy telechelic PCOE precursor determined also from NMR spectroscopy (Table 1).

The monomodality of the block polymer products observed in the SEC chromatograms in all cases suggests the absence of adventitious initiation (Figure 3). The chromatograms show a monotonic decrease in elution volume upon increasing w_L consistent with increasing molecular weight. Also, the PDIs relative to polystyrene standards decrease with increasing w_L (see Table 2). The PCOE homopolymers exhibit PDIs approaching the most probable distribution consistent with extensive chain transfer (see Table 1). Contrarily, Sn(Oct)$_2$-catalyzed **LA** polymerization can provide PLA segments with relatively low PDI. The monotonic decrease in PDI upon increasing w_L suggests that the PLA blocks are significantly less polydisperse than the macroinitiator.[22] Indeed, several samples of PLA synthesized under identical conditions using **C2B** as an initiator resulted in PDI values of 1.1.[23]

The retention time on the SEC columns correlates directly with hydrodynamic volume. As such, the subtle disparity between the relative shifts in elution volume in the SEC chromatograms accentuates the difference in hydrodynamic volume of block polymers with different architectures. The magnitude of elution volume change with increasing molecular weight becomes progressively less pronounced as the number of PLA arms increases (i.e., linear, H-shaped, and arachnearm), consistent with smaller hydrodynamic volume for branched samples compared with linear polymers of equal molecular mass.[24] The absolute molecular weights were measured using SEC with a MALLS detector. The dn/dc required for accurate molecular weight analysis was calculated for a set of PCOE homopolymers assuming 100% mass elution (dn/dc_{PCOE} = 0.11 mL g^{-1} in THF at 30 °C; see Supporting Information). The dn/dc for PLA in THF was determined by Dorgan and co-workers (dn/dc_{PLA} = 0.042 in THF at 30 °C).[25] The composition dependence of the dn/dc in the copolymers was calculated using eq 1.[26] The values of dn/dc tabulated in Table 2 were used to extract the molar masses from the MALLS detector on the SEC. The molar mass of the block polymers determined from SEC−MALLS agrees fairly well with the values calculated from end-group analysis of the telechelic PCOE precursors combined with the composition determined by ^{1}H NMR spectroscopy.

$$\mathrm{d}n/\mathrm{d}c_{AB} = \sum_i w_i(\mathrm{d}n/\mathrm{d}c)_i \qquad (1)$$

The SEC data are consistent with the absence of adventitious initiator and the increase in molecular weight with increased **LA** concentration. However, we cannot unambiguously ascertain

Table 2. Molecular Characteristics of Block Copolymers

sample ID	M_n[a](NMR) (kg mol^{-1})	M_n/PLA arm (kg mol^{-1})	M_n[b](LS) (kg mol^{-1})	PDI[c] (SEC)	w_{PLA}	dn/dc[d] (mL/g)
HO−C−OH Precursor **6**: M_n(NMR) = 22.5 kg mol^{-1}; PDI = 1.70						
9a: LCL [4−22−4]	30.1	4.1	29.5	1.52	0.27	0.086
9b: LCL [10−22−10]	41.1	9.6	40.8	1.37	0.46	0.074
9c: LCL [21−22−21]	64.1	21.1	64.0	1.27	0.66	0.063
9d: LCL [62−22−62]	146	61.8	124	1.30	0.85	0.051
HO_2−C−OH_2 Precursor **7**: M_n(NMR) = 22.8 kg mol^{-1}; PDI = 1.71						
10a: L_2CL_2 [2_2−23−2_2]	29.5	1.8	33.5	1.57	0.26	0.087
10b: L_2CL_2 [5_2−23−5_2]	40.8	4.6	45.2	1.38	0.46	0.074
10c: L_2CL_2 [10_2−23−10_2]	64.5	10.5	64.2	1.23	0.66	0.062
10d: L_2CL_2 [30_2−23−30_2]	144	30.3	129	1.13	0.85	0.051
HO_4−C−OH_4 Precursor **8**: M_n(NMR) = 27.7 kg mol^{-1}; PDI = 1.88						
11a: L_4CL_4 [1_4−27−1_4]	32.7	0.7	32.9	1.62	0.19	0.090
11b: L_4CL_4 [3_4−27−3_4]	47.3	2.6	44.6	1.49	0.44	0.075
11c: L_4CL_4 [6_4−27−6_4]	74.5	6.0	72.3	1.31	0.65	0.063
11d: L_4CL_4 [19_4−27−19_4]	175	18.5	164	1.14	0.85	0.051

[a] Calculated using the M_n (from NMR) for the homopolymer PCOE precursor combined with the relative integral ratios of the respective repeat units in the ^{1}H NMR spectra. [b] Measured using a light scattering detector on an SEC with THF eluant at 30 °C. [c] Measured using an RI detector on an SEC with $CHCl_3$ eluant at 35 °C. [d] Calculated from the THF SEC analysis using the dn/dc value for PCOE (0.11 mL/g) and weight fraction of the two components according to eq 1.

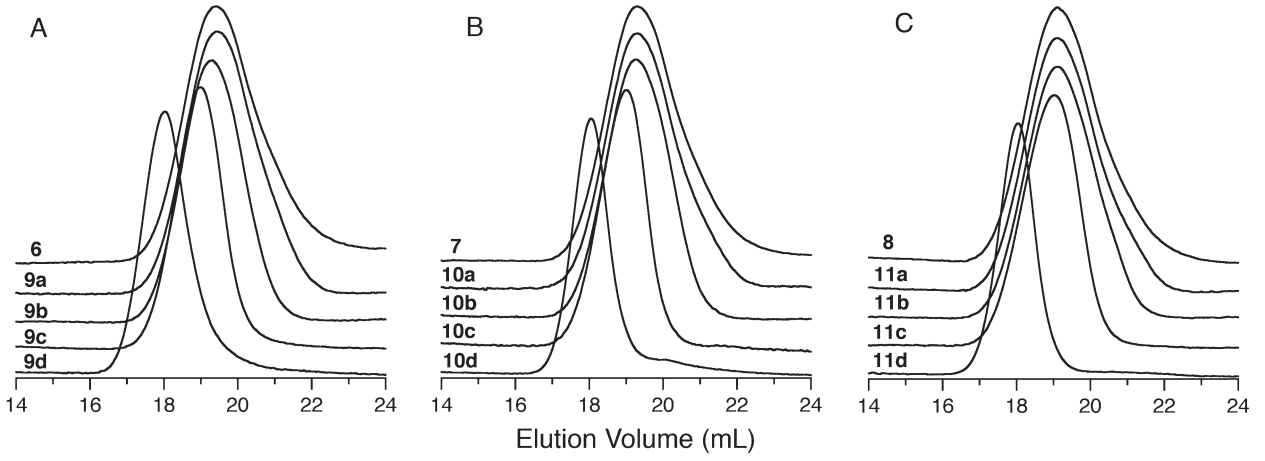

Figure 3. SEC chromatograms for the PCOE homopolymers and block copolymer derivatives having (A) linear [**6**, **9a**−**d**] (B) H-shaped [**7**, **10a**−**d**] and (C) arachnearm [**8**, **11a**−**d**] architectures. The chromatograms in each subset correspond to PCOE homopolymer (**6**, **7**, **8**) and block polymers with PLA weight fractions w_L of approximately 0.25 (**9a**, **10a**, **11a**), 0.45 (**9b**, **10b**, **11b**), 0.65 (**9c**, **10c**, **11c**) and 0.85 (**9d**, **10d**, **11d**) [see Table 2].

the initiating efficacy from SEC. The intended branched architectures are only achievable with quantitative initiating efficiency. This concern is of particular relevance for the bis-MPA based dendritic−linear hybrid macroinitiators, for which the hydroxyl groups are relatively sterically hindered.

Dendritic polyesters based on bis-MPA have been shown to effectively initiate polymerization of D,L-lactide, ε-caprolactone, and other lactone derivatives when catalyzed by $Sn(Oct)_2$, despite the high functional group density.[20b,e,g,27] The initiating efficacy was monitored by ^{1}H NMR spectroscopy for the branched polymers synthesized in this study. Figure 4a shows the full spectrum for the H-shaped copolymer sample **10b**. Again, the repeat unit signals for both components (PCOE and PLA) invariably appear at the same positions regardless of architecture or molar mass. The signals associated with the methylene units adjacent to the hydroxyl groups in the precursors (Figure 2b−d) were monitored and compared with the corresponding signals in the copolymers as highlighted in Figure 4, parts b, c, and d for copolymers **9b**, **10b**, and **11b** with $w_L \approx 0.45$ having linear, H-shaped, and arachnearm architectures, respectively. The clear disappearance of the signal at 4.28 ppm was observed in comparing the linear block polymer (Figure 4b) to the precursor (Figure 2b); this further corroborates the signal being associated with the few PCOE chains having a single lactic acid unit (for discussion of this point, see the Supporting Information). The remaining signal at 4.35 ppm is attributed to the methine unit of PLA chain ends, whereas the signals at 4.55 and 4.68 ppm are assigned to the methylene protons situated at the junction between PCOE and PLA having *trans* and *cis* configurations, respectively. The ratio observed between the PLA end group and the junction protons is consistently 1 to 2, as expected. The methylene proton signals at 4.55 and 4.68 ppm appear as multiplets presumably because of the mixed stereochemistry at the PLA unit adjacent to the junction point. Similar signals were observed for analogous block polymers prepared by a different route.[12]

The ^{1}H NMR spectrum for H-shaped block copolymer **9b** in Figure 4c distinctly illustrates the disappearance of the methylene signal previously adjacent to the hydroxyl groups, which suggests complete initiation from each of the available hydroxyl groups. The signal reemerges downfield as a multiplet centered at 4.22 ppm, consistent with more shielding from the ester. The PLA end-group methine signal once

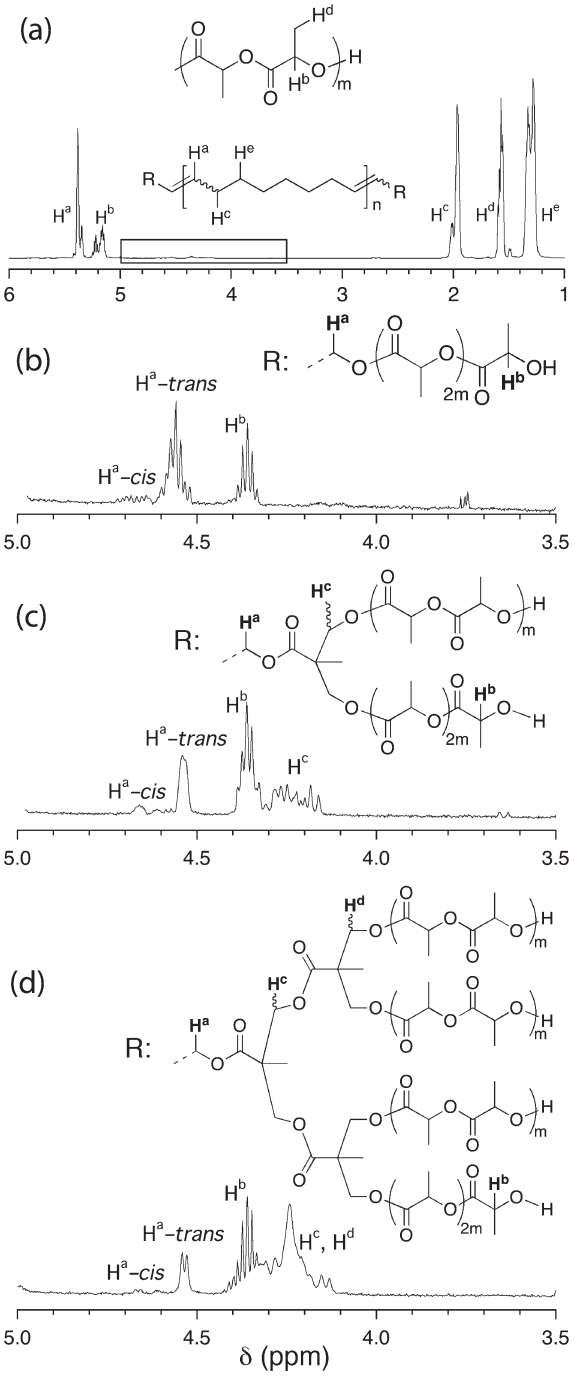

Figure 4. Representative ^{1}H NMR spectrum for L_xCL_x block polymer (a) and insets showing end-group signals for block polymers with (b) linear, (c) H-shaped, and (d) arachnearm architectures.

again emerges at 4.34 ppm with an intensity ratio to the allylic methylene protons of 1:1. A similar trend was observed for the arachnearm block polymers; the signals associated with the hydroxyl-adjacent methylene protons at 3.72 and 3.86 ppm in Figure 2d disappear upon **LA** polymerization and appear as a complex multiplet between 4.1 and 4.4 ppm in Figure 4d. These signals associated with the newly formed ester overlap significantly with the PLA end group (H^b), as well as the methylene protons embedded in the branched structure (H^c in Figure 4d). The integration ratio between the composite signals from 4.1 to 4.4 ppm and the allylic methylene protons at 4.55 and 4.68 ppm is consistently 8:1 as expected from a system in which all the hydroxyls initiated

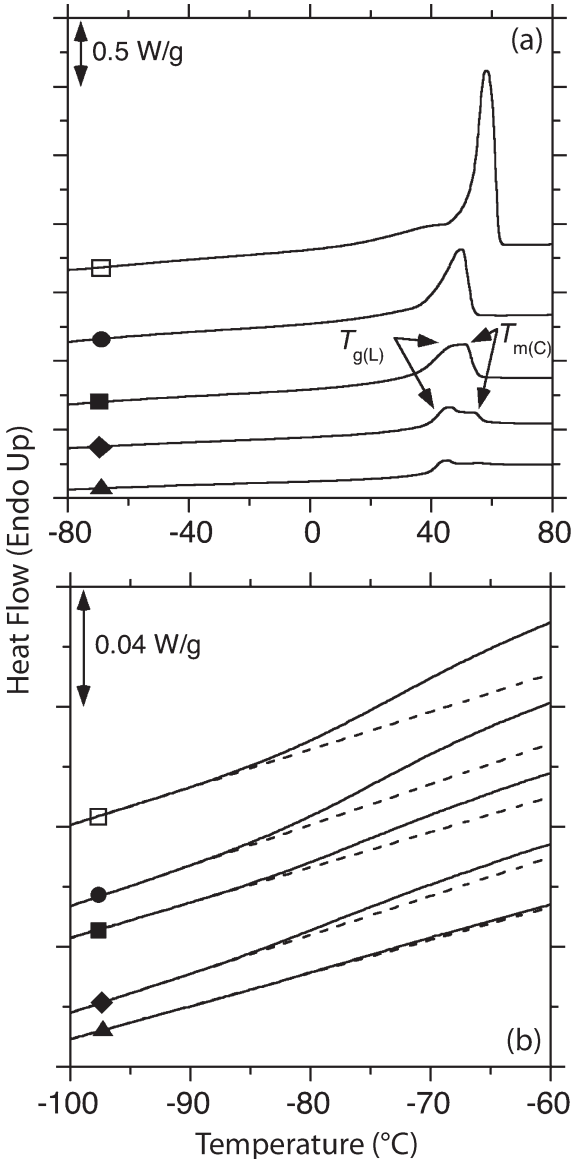

Figure 5. DSC thermograms representing the second heat of the HO−C−OH PCOE homopolymer precursor (□) and linear LCL triblock polymers with PLA weight fractions (w_L) of 0.25 [**9a**] (●), 0.45 [**9b**] (■), 0.65 [**9c**] (◆), and 0.85 [**9d**] (▲). Part a: thermograms from −80 to +80 °C. Part b: magnified portion of thermograms highlighting $T_{g,C}$.

LA polymerization *and* the branched polyester structure remains in tact, suggesting imperceptible transesterification of this sterically hindered unit. This set of data provides compelling evidence that is consistent with the polymer samples exhibiting the branched architectures depicted in Figure 1.

Thermal Characteristics. PCOE homopolymer is a semicrystalline material at ambient temperatures under most conditions with a melting temperature ($T_{m,C}$) near 55 °C.[28] Polymerization of racemic **LA** results in amorphous PLA with a glass transition temperature ($T_{g,L}$) near 50 °C. Figure 5a,b shows the differential scanning calorimetry (DSC) thermograms for the PCOE homopolymer precursor and linear block copolymers with various compositions upon heating from −120 to +120 °C.[29] The melting transition for the PCOE homopolymer occurs at ≈55 °C and the melting enthalpy corresponds to a degree of crystallinity (X_C) equal to 31% as calculated from $X_C = \Delta H_m/\Delta H_m^0$ ($\Delta H_m^0 = 216$ J/g).[18] The glass transition temperature of the HO−C−OH PCOE ($T_{g,C}$) homopolymer occurs at −72 °C as evident from

the top profile in the magnified portion of the thermograms (Figure 5b). The glass transition temperature of the PLA ($T_{g,L}$) in the block polymers occurs between 35 and 40 °C and appears to overlap with the $T_{m,C}$ during heating at 10 °C min^{-1}. The relative invariability and well-separated T_g of each component suggests microphase separation throughout the chosen composition range, consistent with our previous report.[12] The relative magnitude of the glass transition for the two components is consistent with the compositional changes determined from SEC and ^{1}H NMR spectroscopy summarized previously. Figure 5b accentuates the variation in $T_{g,C}$ magnitude with dashed lines added to fit the linear baseline signal at temperatures below $T_{g,C}$. The vertical distance between the dashed extrapolation of the baseline signal and the experimental data at temperatures greater than $T_{g,C}$ provides an estimate of the relative magnitude of the transition and is consistent with the composition.

Conclusions

Well-defined block polymers having various architectures were prepared by combining ROMP of *cis*-cyclooctene and ROTEP of D,L-lactide. ROMP was first performed separately with three newly developed acyclic monounsaturated CTAs bearing either two, four, or eight hydroxyl groups with the functionality governing the ultimate molecular architecture of the block polymer. Subsequent polymerization of D,L-lactide resulted in linear, H-shaped and arachnearm shaped block polymer, respectively, with the soft semicrystalline PCOE tethered on either end by glassy PLA segments. This has particular relevance in developing nanostructured materials based on the ease with which the molecular weights are controlled, the vast array of monomers that could potentially be incorporated using these two mechanisms, and the potential for meticulous control over molecular architecture. The ability to independently manipulate these variables allows specific tailoring of morphological and mechanical characteristics. The consequences of molecular architecture and crystallinity on the self-assembly behavior of these block polymers are currently being explored.

Acknowledgment. This work was funded by The National Science Foundation (DMR-0605880 and DMR 1006370). We thank Mark Amendt and Shingo Kobayashi for helpful discussions during manuscript preparation and acknowledge support from a fellowship awarded by the UMN Department of Chemistry. B.M.C gratefully acknowledges the Office of the Dean at Luther College for financial support of a sabbatical leave of absence. We are grateful to Prof. Timothy P. Lodge for use of the SEC−MALLS instrument.

Supporting Information Available: Text giving experimental details, structural diagrams of the compounds, figures showing ESI mass spectrum of compound **1**, ^{1}H (1D and COSY) and ^{13}C NMR spectra, and IR spectra of all chain transfer agents, and a table of molecular characteristics and d*n*/d*c* values for different homopolymer PCOE samples. This material is available free of charge via the Internet at http://pubs.acs.org.

Note Added after ASAP Publication. This article posted ASAP on September 1, 2010. Scheme 1 has been revised. The correct version posted on September 7, 2010.

References and Notes

(1) Yagci, Y.; Tasdelen, M. A. *Prog. Polym. Sci.* **2006**, *31*, 1133–1170.
(2) (a) Matyjaszewski, K.; Xia, J. *Chem. Rev.* **2001**, *101*, 2921–2990. (b) Hawker, C. J.; Bosman, A. W.; Harth, E. *Chem. Rev.* **2001**, *101*, 3661–3688. (c) Dechy-Cabaret, O.; Martin-Vaca, B.; Bourissou, D. *Chem. Rev.* **2004**, *104*, 6147–6176. (d) Kamber, N. E.; Jeong, W.; Waymouth, R. M.; Pratt, R. C.; Lohmeijer, B. G. G.; Hedrick, J. L. *Chem. Rev.* **2007**, *107*, 5813–5840. (e) Bielawski, C. W.; Grubbs, R. H. *Prog. Polym. Sci.* **2007**, *32*, 1–29.
(3) (a) Bielawski, C. W.; Morita, T.; Grubbs, R. H. *Macromolecules* **2000**, *33*, 678–680. (b) Bielawski, C. W.; Louie, J.; Grubbs, R. H. *J. Am. Chem. Soc.* **2000**, *122*, 12872–12873. (c) Maughon, B. R.; Morita, T.; Bielawski, C. W.; Grubbs, R. H. *Macromolecules* **2000**, *33*, 1929–1935. (d) Mahanthappa, M. K.; Bates, F. S.; Hillmyer, M. A. *Macromolecules* **2005**, *38*, 7890–7894. (e) Myers, S. B.; Register, R. A. *Macromolecules* **2008**, *41*, 5283–5288. (f) Katayama, H.; Fukuse, Y.; Nobuto, Y.; Akamatsu, K.; Ozawa, F. *Macromolecules* **2003**, *36*, 7020–7026. (g) Katayama, H.; Yonezawa, F.; Nagao, M.; Ozawa, F. *Macromolecules* **2002**, *35*, 1133–1136. (h) Matson, J. B.; Grubbs, R. H. *Macromolecules* **2008**, *41*, 5626–5631.
(4) (a) Abetz, V.; Simon, P. F. W. *Adv. Polym. Sci.* **2005**, *189*, 125–212. (b) Bates, F. S.; Fredrickson, G. H. *Annu. Rev. Phys. Chem.* **1990**, *41*, 525–557. (c) Leibler, L. *Prog. Polym. Sci.* **2005**, *30*, 898–914.
(5) (a) Lee, C.; Gido, S. P.; Poulos, Y.; Hadjichristidis, N.; Tan, N. B.; Trevino, S. F.; Mays, J. W. *J. Chem. Phys.* **1997**, *107*, 6460–6469. (b) Gido, S. P.; Lee, C.; Pochan, D. J.; Pispas, S.; Mays, J. W.; Hadjichristidis, N. *Macromolecules* **1996**, *29*, 7022–7028. (c) Beyer, F. L.; Gido, S. P.; Uhrig, D.; Mays, J. W.; Tan, N. B.; Trevino, S. F. *J. Polym. Sci., Part B: Polym. Phys.* **1999**, *37*, 3392–3400. (d) Weidisch, R.; Gido, S. P.; Uhrig, D.; Iatrou, H.; Mays, J.; Hadjichristidis, N. *Macromolecules* **2001**, *34*, 6333–6337. (e) Yang, L. Z.; Gido, S. P.; Mays, J. W.; Pispas, S.; Hadjichristidis, N. *Macromolecules* **2001**, *34*, 4235–4243. (f) Lee, C.; Gido, S. P.; Poulos, Y.; Hadjichristidis, N.; Tan, N. B.; Trevino, S. F.; Mays, J. W. *Polymer* **1998**, *39*, 4631–4638. (g) Buzza, D. M. A.; Fzea, A. H.; Allgaier, J. B.; Young, R. N.; Hawkins, R. J.; Hamley, I. W.; McLeish, T. C. B.; Lodge, T. P. *Macromolecules* **2000**, *33*, 8399–8414.
(6) (a) Hadjichristidis, N.; Pitsikalis, M.; Iatrou, H. *Adv. Polym. Sci.* **2005**, *189*, 1–124. (b) Hadjichristidis, N.; Poulos, Y.; Avgeropoulos, A. *Macromol. Symp.* **1998**, *132*, 207–220.
(7) Sill, K.; Emrick, T. *J. Polym. Sci., Part A: Polym. Chem.* **2005**, *43*, 5429–5439.
(8) Ekin, A.; Webster, D. C. *Macromolecules* **2006**, *39*, 8659–8668.
(9) Han, D.-H.; Pan, C.-Y. *J. Polym. Sci., Part A: Polym. Chem.* **2006**, *44*, 2794–2801.
(10) Liu, J.; Li, J.; Xie, M.; Ding, L.; Yang, D.; Zhang, L. *Polymer* **2009**, *50*, 5228–5235.
(11) Coulembier, O.; Kiesewetter, M. K.; Mason, A.; Dubois, P.; Hedrick, J. L.; Waymouth, R. M. *Angew. Chem., Int. Ed.* **2007**, *46*, 4719–4721.
(12) Pitet, L. M.; Hillmyer, M. A. *Macromolecules* **2009**, *42*, 3674–3680.
(13) Hillmyer, M. A.; Nguyen, S. T.; Grubbs, R. H. *Macromolecules* **1997**, *30*, 718.
(14) (a) Hillmyer, M. A.; Grubbs, R. H. *Macromolecules* **1993**, *26*, 872–874. (b) Bielawski, C. W.; Scherman, O. A.; Grubbs, R. H. *Polymer* **2001**, *42*, 4939–4945.
(15) Bielawski, C. W.; Benitez, D.; Morita, T.; Grubbs, R. H. *Macromolecules* **2001**, *34*, 8610–8618.
(16) Hillmyer, M. A.; Grubbs, R. H. *Macromolecules* **1995**, *28*, 8662–8667.
(17) Polymerization of cyclooctadiene can yield functionality $F_n < 2$ due to the presence of adventitious CTA vinylcyclohexene in the monomer feedstock (see: Ji, S.; Hoye, T. R.; Macosko, C. W. *Macromolecules* **2004**, *37*, 5485–5489) .
(18) Scherman, O. A.; Kim, H. M.; Grubbs, R. H. *Macromolecules* **2002**, *35*, 5366–5371.
(19) Ihre, H.; Hult, A.; Frechet, J. M. J.; Gitsov, I. *Macromolecules* **1998**, *31*, 4061–4068.
(20) (a) Trollsas, M.; Kelly, M. A.; Claesson, H.; Siemens, R.; Hedrick, J. L. *Macromolecules* **1999**, *32*, 4917–4924. (b) Trollsas, M.; Hedrick, J. L.; Mecerreyes, D.; Dubois, P.; Jérôme, R.; Ihre, H.; Hult, A. *Macromolecules* **1998**, *31*, 2756–2763. (c) Trollsas, M.; Hedrick, J. L. *Macromolecules* **1998**, *31*, 4390–4395. (d) Jérôme, R.; Mecerreyes, D.; Tian, D.; Dubois, P.; Hawker, C. J.; Trollsas, M.; Hedrick, J. L. *Macromol. Symp.* **1998**, *132*, 385–403. (e) Atthoff, B.; Trollsas, M.; Claesson, H.; Hedrick, J. L. *Macromol. Chem. Phys.* **1999**, *200*, 1333–1339. (f) Trollsas, M.; Hawker, C. J.; Remenar, J. F.; Hedrick, J. L.; Johansson, M.; Ihre, H.; Hult, A. *J. Polym. Sci., Part A: Polym. Chem.* **1998**, *36*, 2793–2798. (g) Trollsas, M.; Atthoff, B.; Claesson, H.; Hedrick, J. L. *J. Polym. Sci., Part A: Polym. Chem.* **2004**, *42*, 1174–1188. (h) Trollsas, M.; Claesson, H.; Atthoff, B.; Hedrick, J. L. *Angew. Chem., Int. Ed.* **1998**, *37*, 3132–3136.
(21) This conclusion is in line with observations made by the R. H. Grubbs research group. Grubbs, R. H. Personal communication .
(22) Hamley, I. W. *Dev. Block Copolym. Sci. Technol.* **2004**, 1–29.
(23) Three PLA samples were prepared (**C2B** initiator, $Sn(Oct)_2$ catalyst) with degrees of polymerization ([**LA**]/[**C2B**]) equal to 50, 100,

and 200 having PDIs measured in chloroform at 35 °C of 1.13, 1.14, and 1.10, respectively.
(24) (a) Jeong, M.; Mackay, M. E.; Vestberg, R.; Hawker, C. J. *Macromolecules* **2001**, *34*, 4927–4936. (b) Roovers, J.; Toporowski, P. M. *J. Polym. Sci., Part B: Polym. Phys.* **1980**, *18*, 1907–1917. (c) Hadjichristidis, N.; Roovers, J. E. L. *J. Polym. Sci., Part B: Polym. Phys.* **1974**, *12*, 2521–2533. (d) Mourey, T. H.; Turner, S. R.; Rubinstein, M.; Frechet, J. M. J.; Hawker, C. J.; Wooley, K. L. *Macromolecules* **1992**, *25*, 2401–2406.
(25) Dorgan, J. R.; Janzen, J.; Knauss, D. M.; Hait, S. B.; Limoges, B. R.; Hutchinson, M. H. *J. Polym. Sci., Part B: Polym. Phys.* **2005**, *43*, 3100–3111.
(26) Medrano, R.; Laguna, M. T. R.; Saiz, E.; Tarazona, M. P. *Phys. Chem. Chem. Phys.* **2003**, *5*, 151–157.
(27) Trollsas, M.; Claesson, H.; Atthoff, B.; Hedrick, J. L.; Pople, J. A.; Gast, A. P. *Macromol. Symp.* **2000**, *153*, 87–108. (b) Trollsas, M.; Hedrick, J. L. *J. Am. Chem. Soc.* **1998**, *120*, 4644–4651. (c) Trollsas, M.; Hedrick, J.; Mecerreyes, D.; Jérôme, R.; Dubois, P. *J. Polym. Sci., Part A: Polym. Chem.* **1998**, *36*, 3187–3192. (d) Trollsas, M.; Hedrick, J. L.; Mecerreyes, D.; Dubois, P.; Jérôme, R.; Ihre, H.; Hult, A. *Macromolecules* **1997**, *30*, 8508–8511.
(28) Schneider, W. A.; Müller, M. F. *J. Mol. Catal.* **1988**, *46*, 395–403.
(29) Only a select portion of the thermograms are displayed in Figure 5 to accentuate the sections in which the relevant thermal transitions occur. The heating portion represents the second heat after the thermal history of the samples was standardized by first heating to 160 °C followed by cooling to −120 at 10 °C min^{-1} and second heating to +120 at 10 °C min^{-1}